Heliyon 10 (2024) e33788

Contents lists available at ScienceDirect

Heliyon

journal homepage: www.cell.com/heliyon

Research article

Drug delivery particles for targeted imaging-guided photothermal/chemotherapy synergy cancer therapy

Shenglong Shi [a,1], Yingying Zhang [b,c], Jian Huang [b,d,1], Zhengji Wang [b], Weiyang Lv [a], Xing Li [a], Ying Wang [a], Chunxin Huang [a], Huilin Liu [a,*]

[a] Department of Ultrasound, The Second Affiliated Hospital of Qiqihar Medical University, China
[b] Qiqihar Medical University, Qiqihar, China
[c] MinKang Hospital of Qiqihar, Qiqihar, China
[d] West Coast Second Hospital of Qingdao University Medical Group

ARTICLE INFO

Keywords:
Pancreatic cancer
Ultrasound
Superparamagnetic iron oxide
Perfluoropentane
Doxorubicin

ABSTRACT

The early stage of pancreatic cancer is asymptomatic and the treatment effect is not ideal. The progression to the advanced stage leads to a close relationship between mortality and morbidity. Therefore, there is an urgent need to develop precise and efficient therapeutic strategies to combat pancreatic cancer. In this study, we introduce a near-infrared (NIR) targeted drug delivery nanoparticle for ultrasound (US) imaging to guide magnetothermal/chemotherapy synergistic treatment of pancreatic cancer. Carboxylated polylactic acid (PLGA-PEG-COOH) serves as the structure of the nanoparticles, specifically binding the RGD cyclic peptide for pancreatic cancer targeting activity and promoting tumor aggregation of the nanoparticles. NIR-induced superparamagnetic iron oxide (SPIO) nanoparticles convert near-infrared light into thermal energy, triggering vaporization of perfluoropentane (PFH) droplets to generate PFH bubbles that enhance US imaging and help load doxorubicin (DOX), which are released from nanoparticles. SPIO can also be used for thermal ablation of tumors to improve therapeutic effect in treating pancreatic cancer. The results show that the targeted particles mediated by NIR have the characteristics of targeted drug delivery imaging. The microspheres exhibit strong acoustic and near-infrared responsiveness. Cell proliferation experiments showed that IR-mediated PFH-DOX@PLGA/SPIO-RGD NPs (RNPs) had a higher inhibitory effect on cell proliferation. Animal experiments have shown that RNPS can accumulate highly in the tumor area and show good therapeutic effect. In conclusion, this nanotherapeutic particle is a very promising targeted image-guided photothermal/chemotherapeutic synergistic tumor therapy strategy.

1. Introduction

Pancreatic cancer is a fatal solid malignant tumor with strong invasiveness and poor prognosis, with a five-year survival rate of only about 5 % [1]. However, because there are no identifiable symptoms or signs in the early stages of pancreatic cancer, many patients are already at an advanced stage when they seek treatment and have metastasized to other organs, making them unsuitable for surgical

* Corresponding author. The Second Affiliated Hospital of Qiqihar Medical University, Qiqihaer, 101006, China.
E-mail address: L191747912@163.com (H. Liu).
[1] These authors contributed equally to this work.

https://doi.org/10.1016/j.heliyon.2024.e33788
Received 26 February 2024; Received in revised form 25 June 2024; Accepted 26 June 2024
Available online 27 June 2024

resection. Coupled with the systemic toxicity of chemotherapy drugs and the multidrug resistance of pancreatic cancer, the effectiveness of conventional treatments such as radiotherapy and chemotherapy is greatly reduced [2,3]. Therefore, the development of new diagnostic and therapeutic methods is crucial to improve the prognosis of patients with pancreatic cancer. In recent years, nanodrug-carrying systems have been widely used in cancer diagnosis and treatment research and have shown good application prospects [4,5]. Nano drug-carrying systems can not only improve the utilization rate of hydrophobic drugs, increase the accumulation of drugs in the lesion tissue, and improve the therapeutic effect, but can also be combined with contrast agents and other treatment methods to achieve integrated diagnosis and treatment [6]. Photothermal therapy is a physical therapy method that uses near-infrared light to generate heat energy to kill tumor cells. It has the advantages of small invasion, safety, and high efficiency [7]. The structure and function of new blood vessels in tumor tissue are abnormal, and the heat generated during treatment is not easily taken away by blood circulation, while normal tissue can dissipate heat from the body by accelerating blood flow [8,9]. Therefore, photothermal therapy is not suitable for There is less damage to normal tissue. However, the heat generated during treatment is unevenly distributed within the tumor, and some tumor cells still survive after treatment, causing disease recurrence and affecting the therapeutic effect [10].

Doxorubicin hydrochloride (DOX) belongs to the first-generation anthracycline antibiotics and is a water-soluble anticancer drug with a strong therapeutic effect on many cancers [11]. Although doxorubicin has good efficacy against cancer, the systemic dispersion caused by its administration may cause some adverse side effects, including hepatic accumulation, rapid clearance, and cardiomyopathy. To eliminate or reduce these side effects, a range of drug delivery systems need to be developed. A large number of studies have shown that single-drug treatment cannot achieve the desired effect, which may be related to individual differences, tumor metastasis, drug resistance, and other factors [12]. Collaborative treatment based on multiple treatment modalities is superior in cancer treatment. Among many nanocarriers, the polymer poly (lactide-*co*-glycolic acid) (PLGA) has good biodegradability and biocompatibility, and its surface can be easily modified with other ligands or functional groups and has been widely studied [13,14]. SPIO is an inorganic photothermal material and MRI T_2-weighted contrast agent that has been certified by the U.S. Food and Drug Administration (FDA) and can be used in clinical research [15,16]. PFH is a fluorocarbon substance with good stability. After phase change, it can significantly improve the contrast of ultrasound imaging, thus enhancing the diagnostic effect of diseases [17]. Therefore, adding photothermal materials to the PLGA drug-loading system to achieve combined chemotherapy and photothermal therapy may be a very potential cancer treatment method.

In this study, PLGA was used as a carrier, which contained the chemotherapy drug doxorubicin (DOX), oleic acid-modified SPIO, and the phase change material perfluoropentane (PFH, with a boiling point of 29 °C), a nano drug-loading system was designed using the double-emulsion solvent evaporation method (W/O/W). Under the irradiation of the near-infrared laser, this targeted nano-drug-carrying system showed good photothermal effects, producing local hyperthermia at the tumor site of tumor-bearing mice, and the generated PFH bubbles promoted the release of DOX, realizing chemotherapy/photothermal treatment. Integration. At the same time, PFH bubbles achieve ultrasound imaging enhancement. Realize the diagnosis of pancreatic cancer on photoacoustic dual-modal imaging and guide tumor treatment. In this study, various elements with good biological safety were integrated into a nano-system, so that the functions of each component complement each other, and finally achieved chemotherapy/photothermal therapy synergistic treatment, which is expected to integrate the diagnosis and treatment of pancreatic cancer. Provide new methods.

2. Materials and methods

2.1. Materials

Oleic acid-modified SPIO nanoparticles (28 mg/mL, d = 20 nm), carboxylated polylactic-*co*-glycolic acid (PLGA), and doxorubicin (DOX) were purchased from Aladdin (Shanghai, China). Propidium iodide (PI) and CCK-8 kits were obtained from Sigma (New Jersey, USA). Acridine orange (AO-ethidium bromide EB) kit was purchased from Coolaber (Beijing, China). Annexin V-FITC kit was purchased from KeyGEN (Nanjing, China). High glucose medium (DMEM) and fetal calf serum were purchased from Hyclone (USA).

2.2. Synthesis of PFH-DOX@PLGA/SPIO-RGD NPs

The carboxylated PLGA (150 mg) was fully dissolved in 4 mL dichloromethane ($CHCl_2$), followed by the addition of 100 μL PFH, DOX (4 mg), and SPIO (10 mg). The mixed solution was made into a primary emulsion utilizing an ultrasonic cell splitter. The primary emulsion was poured into 10 mL of PVA solution (5 % ， w/v) and the second emulsion was made by re-acoustic vibration of the probe. Then, the second emulsion was added to 20 mL of isopropanol solution (2 %, w/v) and left at 4 °C for 8 h to fully volatilize $CHCL_2$. Finally, the final solution was collected after high-speed centrifugation for 7 min and stored at 4 °C.

RGD-targeted PFH-DOX@PLGA/SPIO NPs (RNPS)were prepared by carbodiimide method. The above solutions were dispersed in MES buffer (0.1 mol/L, pH 5.5). EDC and NHS (molar ratio = 1:3) were added as activator solutions and stirred for 4 h at room temperature. After washing three times by thorough centrifugation using PBS, the activated solution was redispersed in MES buffer (0.1 mol/L, pH 8). Then, excess RGD peptide was added and the reaction was allowed for 12 h at room temperature. Finally, the final RNPs were obtained after washing with PBS by sufficient centrifugation to remove unbound RGD.

2.3. Characterization of RNPs

The morphology of RNPS was observed by scanning electron microscope (SEM, Hitachi Regulus 8100). Particle size distribution

and ZETA potential were assessed by Malvern Zetasizer. The NPs were dispersed in PBS solution and stored at 4 °C. They were removed at 5, 10, and 15 days, respectively, and the morphology and size changes were observed by SEM. The samples were analyzed by X-ray diffraction (XRD) at room temperature. The FITC-labeled goat anti-human antibody was incubated for 2 h to assess RGD binding on NPs, and the staining was then visualized under a confocal laser scanning microscope and the fluorescence binding rate was tested using ImageJ.

2.4. Liquid-gas phase transition characteristics in vitro

The liquid-gas phase transition of PFH in NPs was observed on a light microscope. 500 μl RNPS were placed on a slide and irradiated using NIR and the temperature change values were recorded.

2.5. DOX loading and light-controlled in vitro drug release

The DOX-PBS solution (1 mg/mL) was prepared, and the gradient solution was obtained by adding the gradient content of PBS. The standard curve was drawn, and then the encapsulation efficiency and drug loading of DOX were calculated.

ICP-OES(Thermo Fisher iCAP PRO) was used to detect the Fe content in PFH-DOX@PLGA/SPIO-RGD NPs, and the encapsulation rate of SPIO in NPs was calculated.

$$\text{Encapsulation Efficacy}(\%) = \frac{\text{drug mass} - \text{free drug mass}}{\text{drug mass}} \times 100\% \quad (1)$$

$$\text{Drug loading rate}(\%) = \frac{\text{drug mass} - \text{free drug mass}}{\text{drug masstotal sample mass}} \times 100\% \quad (2)$$

The RNPS were transferred to the dialysis bag and placed into 50 mL PBS solution with low-speed stirring. The temperature was heated to 20 °C, 40 °C, and 60 °C, and the absorbance of PBS solution was measured at 2, 4, 8, 12, 24, and 48 h.

The following formula was used to calculate the drug release rate:

$$\text{Drug release rate}(\%) = \frac{\text{drug mass in solution x50}}{\text{drug loading rate}} \times 100\% \quad (3)$$

2.6. Cell culture and animal models

Pancreatic cancer HPAC cells were obtained from the Laboratory of Molecular Imaging, Qiqihar Medical University. Cells were cultured in DMEM medium with high glucose, supplemented with 10 % FBS and 1 % penicillin/streptomycin. The cultures were maintained at 37 °C and 5 % CO_2. Nude mice weighing 15–20 g and aged 4–6 weeks were obtained from the Animal Center of Qiqihar Medical University. HPAC cells were isolated and suspended in cold PBS. The mice were then injected with 1×10^6 cells per mouse into the left armpit. In vivo experiments were conducted once the tumor volume reached 70 mm^3. All animal procedures were carried out in compliance with the Animal Ethics Committee guidelines of Qiqihar Medical University.

2.7. Cell targeting and intracellular drug release assays

First, HPAC cells (1×10^5 cells per well) were seeded at a density of 1×10^5 cells per well in 6-well plates. After 12 h, the culture medium was changed to contain PFH-DOX@PLGA/SPIO NPs and RNPS (60 μg/mL) for another 12 h. After the NIR ($2W/cm^2$) intervention, the fluorescence intensity was observed by laser confocal microscopy. The size of the tumor was measured every three days. The tumor volume (V) was calculated as $V = 0.5 \times \text{length} \times \text{width}^2$. After 15 days, the tumor and major organs were removed for immunohistochemistry and then observed using a light microscope.

2.8. In vivo toxicity and cell proliferation inhibition experiments

The biological safety and killing effect of RNPs on tumor cells were analyzed by CCK-8 assay. First, cells were seeded at a density of 5×10^3 cells per well and cultured in 96-well plates for 12 h. PFH DOX@PLGA/SPIO NPs and RNPs were divided into four groups with or without NIR($2W/cm^2$) mediations, and free DOX was the control group. Then continue to cultivate for 12 h. The dosage for each medication is 50 μg/mL 10 μL of CCK-8 reagent was added to the reaction for 30 min at room temperature. The absorbance at 450 nm was measured using a microplate reader.

Cell viability was calculated using the following formula:

$$\text{Cell viability}\ (\%) = \frac{\text{OD sample} - \text{OD blank}}{\text{OD control} - \text{OD blank}} \times 100\% \quad (4)$$

2.9. Apoptosis analysis

To further analyze whether the inhibition of cell proliferation caused by NIR-irradiated RNPS was associated with the induction of

apoptosis, we used AO/EB staining and flow cytometry for further observation. First, 1×10^5 HPAC cells/well were seeded and cultured in 6-well plates for 12 h. Cultures were continued for 12 h as grouped as described above. Flow cytometry was used to detect cell apoptosis and acridine orange/ethidium bromide (AO/EB) detection kit fluorescence staining.

2.10. In vivo imaging experiments

When the tumor volume reached 200 mm^3, in vivo imaging was conducted. The nude mice bearing the tumor were anesthetized using 1 % sodium pentobarbital. Subsequently, the mice were divided into three groups, each group containing five mice (n = 5). Which were given the same dose of PBS, RNPS, and PFH-DOX@PLGA/SPIO NPs intravenously, respectively. Based on the fluorescence characteristics of DOX itself, RNPs can be used for fluorescence imaging analysis to evaluate the degree of tumor targeting accumulation. Then in vivo fluorescence imaging was performed 2 h before and after RNPs injection. Then, the tumor was irradiated with a near infrared laser with a power of 2 W/cm^2, and the tumor was imaged with HIFU ultrasonic diagnostic instrument.

2.11. Statistical analysis

Each group of experiments was repeated three times. The *t*-test was used for comparison between two groups, and one-way analysis of variance was used for multiple groups. $P < 0.05$ was considered to indicate statistical significance.

3. Results

3.1. Preparation and characterization of RNPS

RNPS with targeted imaging therapy were prepared by stable and mature double emulsion method and carbodiimide method [18]. To summarize, an organic phase consisting of PLGA-PEG-COOH polymer dissolved a solution composed of SPIO particles modified with oleic acid, PFH, and DOX. Following this, the solution underwent phacoemulsification using a probe. The anti-RGD antibody was then coupled to the nanoparticles by coupling the amino group in the RGD to the carboxylate group on the nanoparticle surface (Fig. 1), and uses near-infrared laser irradiation to make the internal PFH phase transition, which increases the echo intensity of US and enables tumor targeted imaging. After further irradiation with near-infrared laser, RNPs breaks and releases internal DOX to achieve

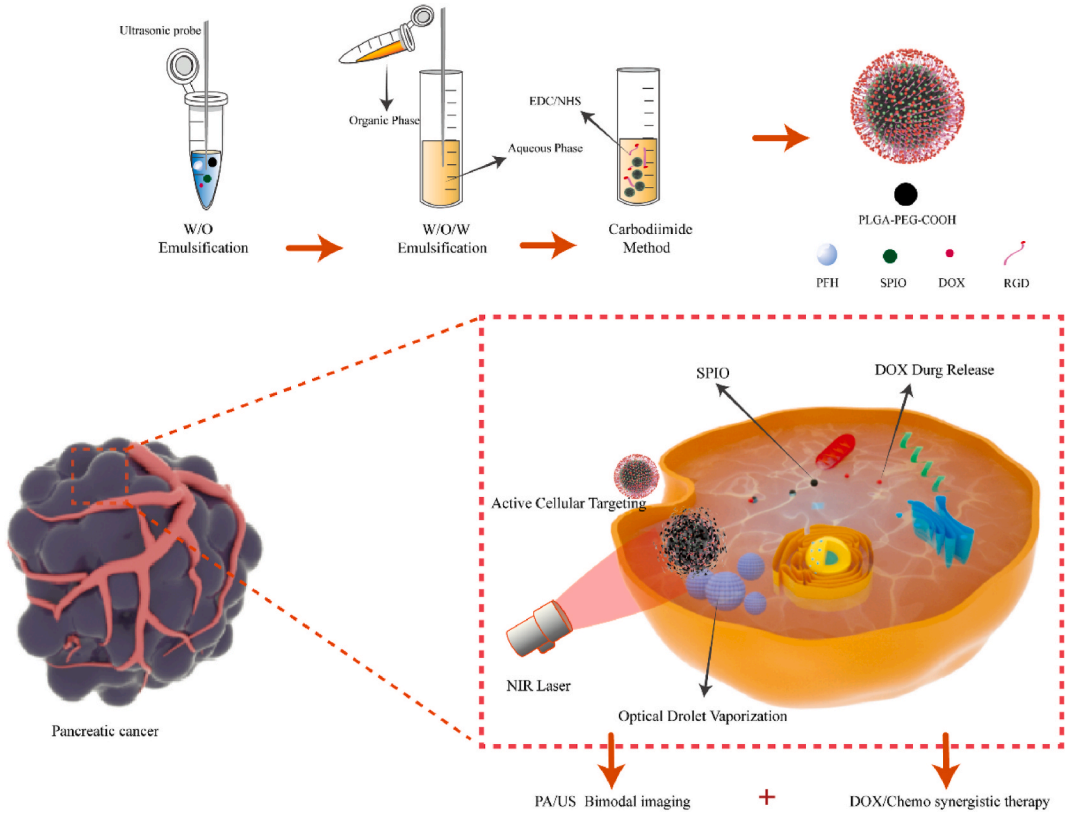

Fig. 1. Schematic of the fabrication principle of the RNPs nanosystem and the process of near-infrared controlled drug delivery, guided photothermal/chemotherapy synergy for cancer treatment, and targeted PA/US imaging.

the purpose of treatment. Models of tumor cells and nanoparticles rendered using C4D.

The RNPS were homogeneous spherical particles observed by SEM (Fig. 2A), with an average diameter of 374.8 nm and Zeta potential of −23.28 mV (Fig. 2B). SEM was further used to assess the stability of RNPS overtime at 4 °C. No significant changes in morphology were observed within 15 days. The results show that the RNPS has good stability (Fig. 2C), which provides a basis for the following biomedical applications.

3.2. RNPS phase analysis

Phase analysis of the RNPS samples was performed using X-ray diffractometer (XRD) to investigate the phase structure. The results are shown in Fig. 3, and the SPIO diffraction peak is consistent with the standard card of iron oxide (JCPDS No. 99-0073). Compared with SPIO, RNPS showed diffraction peaks at 511° and 440°, and no other diffraction peaks were observed, indicating that SPIO may be formed in the internal structure of NPs.

3.3. Validation of the in vitro targeting of RNPS

For nano drug delivery systems, having effective disease targeting is essential to achieve precise drug delivery and imaging-guided therapy [19,20]. Therefore, we determined the binding efficiency of RGD to PFH-DOX@PLGA/SPIO NPs and the cell-targeting behavior of the RNPS. Fig. 4A shows the RNPS containing DOX (red fluorescence), the FITC-labeled secondary antibody (green fluorescence), and the red NPs and the green secondary antibody overlapping, shown as yellow fluorescence. The fluorescence binding rate of the ImageJ test was 98.73 %.

The cell-targeting behavior of the NPs was observed by confocal microscopy of HPAC cells. As shown in Fig. 4B, for HPAC cells, a red fluorescence signal representing DOX-labeled targeting RNPS was observed in the cytoplasm, whereas a weaker red fluorescence signal was found in cells cultured with non-targeting PFH-DOX@PLGA/SPIO NPs, This suggests that RGD peptide surface modification can significantly improve the targeted cellular uptake of NPs. These results suggest that RGD can confer cellular targeting to RNPS for uptake by HPAC cells through active antigen-antibody interactions. Thus, such nanoplatforms offer excellent opportunities for accurate multimodal imaging and efficient collaborative pancreatic cancer therapy.

3.4. Temperature-controlled liquid-gas phase transition process of NPs

To achieve near-infrared light-mediated temperature-controlled drug release of RNPS, we evaluated their liquid-gas phase transition process. First, we investigated the phase transition of NPs irradiated with NIR laser at a power of 2 W/cm^2. As shown in Fig. 5A,

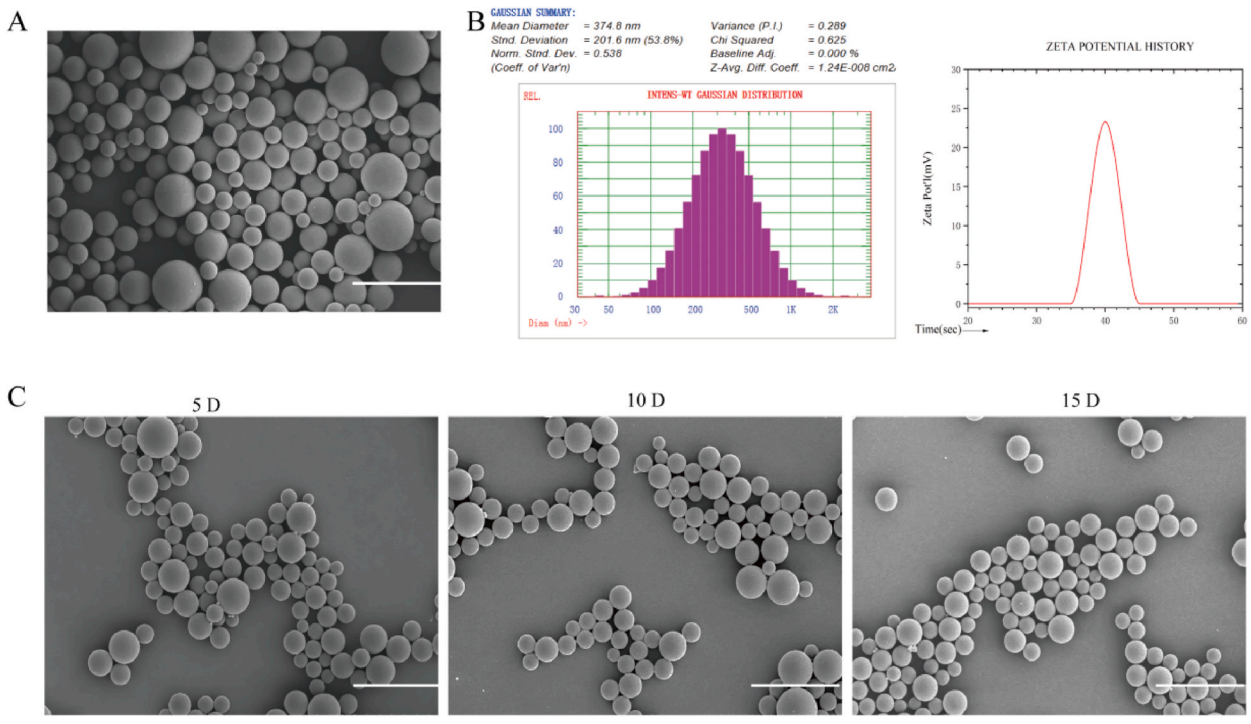

Fig. 2. Characterization and Stability of RNPS. A. SEM of RNPS. B. Hydrated particle size and potential. C. Morphological changes of RNPS at 4 °C in 5, 10 and 15 days. Scale = 1 μm.

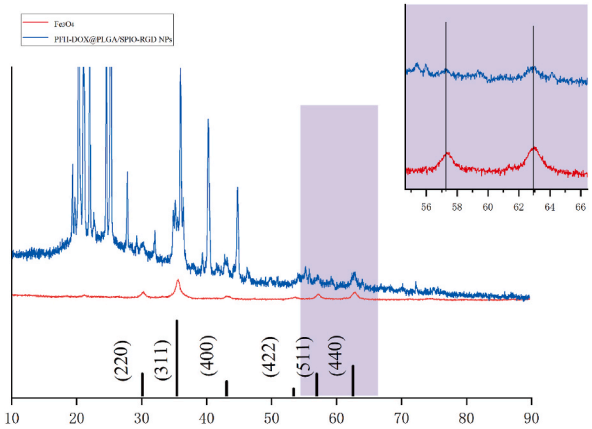

Fig. 3. XRD patterns of SPIO nanoparticles and RNPS.

when the temperature is 20 °C, the NPs are spherical particles with uniform size. When the temperature was 40 °C, only a small amount of NPs gradually transformed into gas microbubbles. The size of the microbubbles increased with increasing temperature, reaching a maximum of around 60 °C (Fig. 5B). These results suggest that the phase transition of RNPS can be controlled by temperature. However, excessive temperatures may cause microbubble rupture.

3.5. Temperature-controlled drug release in vitro

The drug loading and encapsulation efficiency of DOX were 41.5 % and 83.1 %, respectively. The encapsulation efficiency of SPIO was 68.61 ± 2.57 %. Next, temperature-triggered DOX release from NPs was investigated. The cumulative release of DOX was calculated at 2 h. At 20 °C, DOX was released very slowly from the NPs. However, less DOX release from the NPs was observed at 40 °C (Fig. 5C). It is worth mentioning that the cumulative release rate of DOX from RNPS was 85.74 % at 60 °C. Due to the excellent photothermal conversion efficiency of SPIO, the drug release of RNPS increases whenever NIR is irradiated, and the drug release curve flattens when NIR is turned off (Fig. 5D).However, there was no significant change in the release rate of NPs without SPIO. These results indicate that RNPS can be temperature-controlled in response to drug release, thus promoting DOX release from NPs according to the change of temperature.

3.6. Cytotoxicity analysis

PLGA material has high biosafety and biodegradability and is currently the mainstream biodegradable material [21]. As shown in Fig. 6, the cell survival rate of the RNPS group at 24 h did not change significantly with the increase of concentration, indicating that the NPs with PLGA as membrane structure had good biocompatibility. Notably, the NIR-irradiated RNPS group had a significantly lower cell survival rate than the DOX group at 24 h.

3.7. AO/EB fluorescence double staining experiments

To investigate the inhibitory effect of RNPS on cell proliferation, We used DOX, PFH-DOX@PLGA/SPIO NPs, RNPS, and RNPS after NIR irradiation The apoptotic effects on cells were explored by the grouping of NPs. As shown in Fig. 6, compared with PFH-DOX@PLGA/SPIO NPs group, most of the cells in PFH-DOX@PLGA/SPIO NPs group had normal morphology and uniform green cytoplasm, and no obvious apoptosis was observed [22]. The DOX group showed pyknosis and cylindrical cell morphology, and the cell staining was yellow, indicating the generation of apoptosis [23]. The results of IR irradiation of the RNPS group were similar to those of the DOX group. Although there was no targeted modification, it also produced a certain killing effect on cells in the relatively limited environment of the culture dish. The NIR-irradiated RNPS group lost cell morphology and stained orange-red, indicating that most of the cells were apoptotic and only a few cells survived [24].

3.8. Flow cytometry detection

To further investigate whether the NPs inhibited the proliferation of HPAC cells by inducing apoptosis, Annexin V-FITC/PI apoptosis detection kit was used to detect the effect on apoptosis of HPAC cells. As shown in Fig. 7, compared with PFH-DOX@PLGA/SPIO NPs group cultured for 24 h, the RNPS group showed no significant increase in cell apoptosis rate (12.8 %). The apoptosis rate of the DOX group (46.6 %) was lower than that of the IR-irradiated RNPS group (87.4 %). The NPs modified by RGD cyclic peptide showed better performance on the apoptosis of HPAC cells (see Fig. 8).

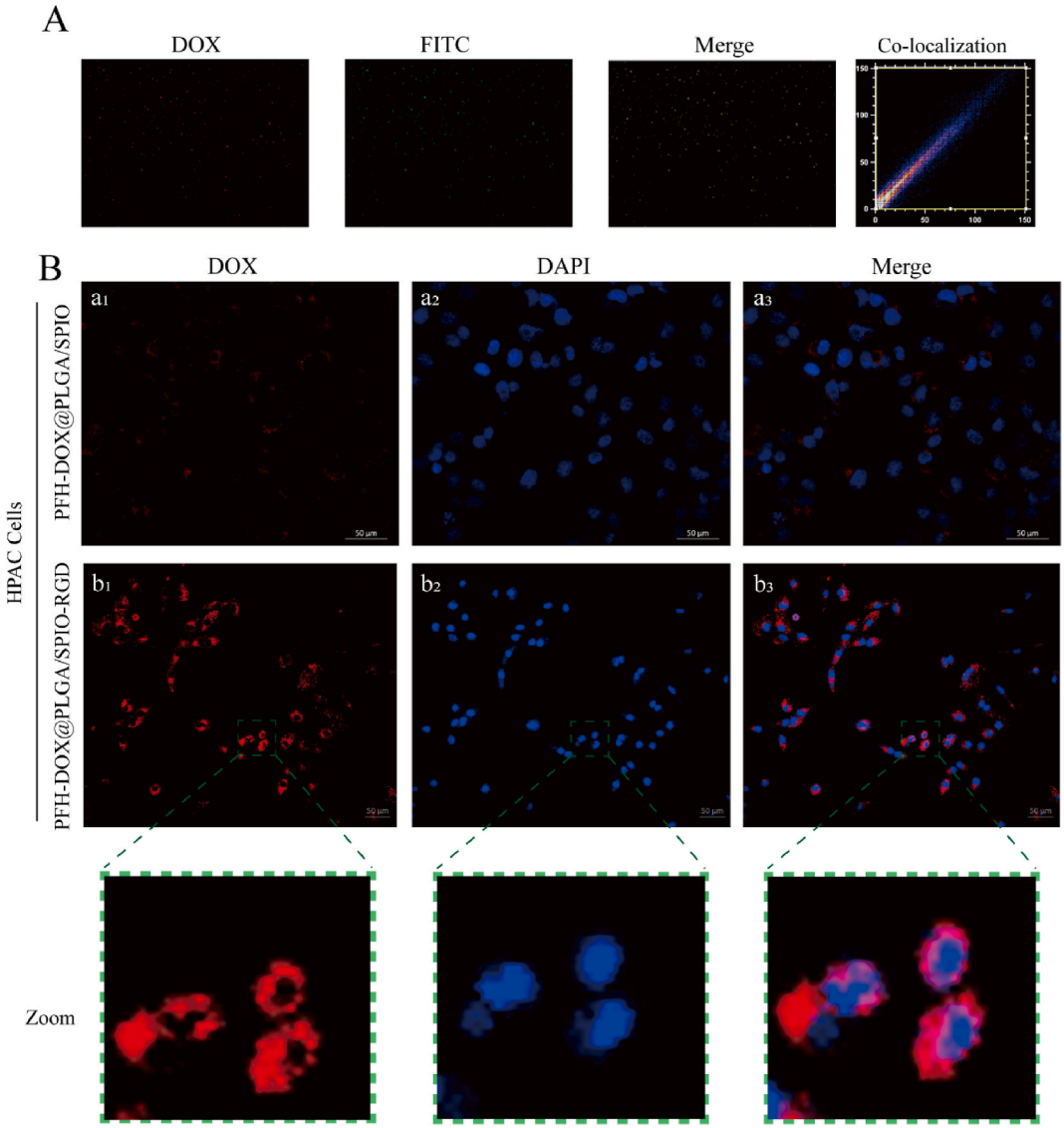

Fig. 4. Cellular targeting studies of RNPS. (A) Fluorescence microscopy image of DOX-containing NPs(red fluorescence) incubated with FITC-labeled goat anti-human antibody (green fluorescence) for 2 h after covalent binding reaction. In Merge, yellow fluorescence represents the overlap of NPs and antibodies. (B) (a1-a3) shows laser confocal microscopy images of HPAC cells incubated with non-targeted NPs for 12 h; (b1-b3) are laser confocal microscopy images of targeted NPs and HPAC cells.

3.9. RNPS in vivo imaging performance

RNPS can be used in the photothermal/chemotherapy synergistic therapy of pancreatic cancer, and the tumor-targeting aggregation of NPs was detected by US and PA imaging. First of all, 15 nude mice were used in the experiment, 14 of which were successfully modeled, one of which had no tumor growth, and the success rate of modeling was 93 %. In the absence of NIR irradiation after NPs injection, there was no significant enhanced echo in the tumor region. After NIR irradiation (2 W/cm^2, 15 min), the echo effect in the tumor area was enhanced, indicating that the phase transition of NPs resulted in the change of acoustic properties under NIR irradiation. NIR continuously irradiates the tumor area to completely phase transform PFH and break the PLGA shell, releasing internal DOX to achieve the purpose of treatment.To verify the distribution of RNPS in vivo, we performed in vivo fluorescence imaging in nude mice. The fluorescence signal gradually appeared in the tumor area after 2 h of injection, and the fluorescence intensity reached a peak after 24 h.

As shown in Fig. 9. C, PFH-DOX@PLGA/SPIO-RGD NPs significantly reduced tumor volume compared with PBS and PFH-DOX@PLGA/SPIO NPs. Targeting ligands accelerates the aggregation of NPs at the tumor site, resulting in strong antitumor activity. In addition, as shown in Fig. 9. D, all nude mice in each group maintained normal weight gain without significant abnormalities.

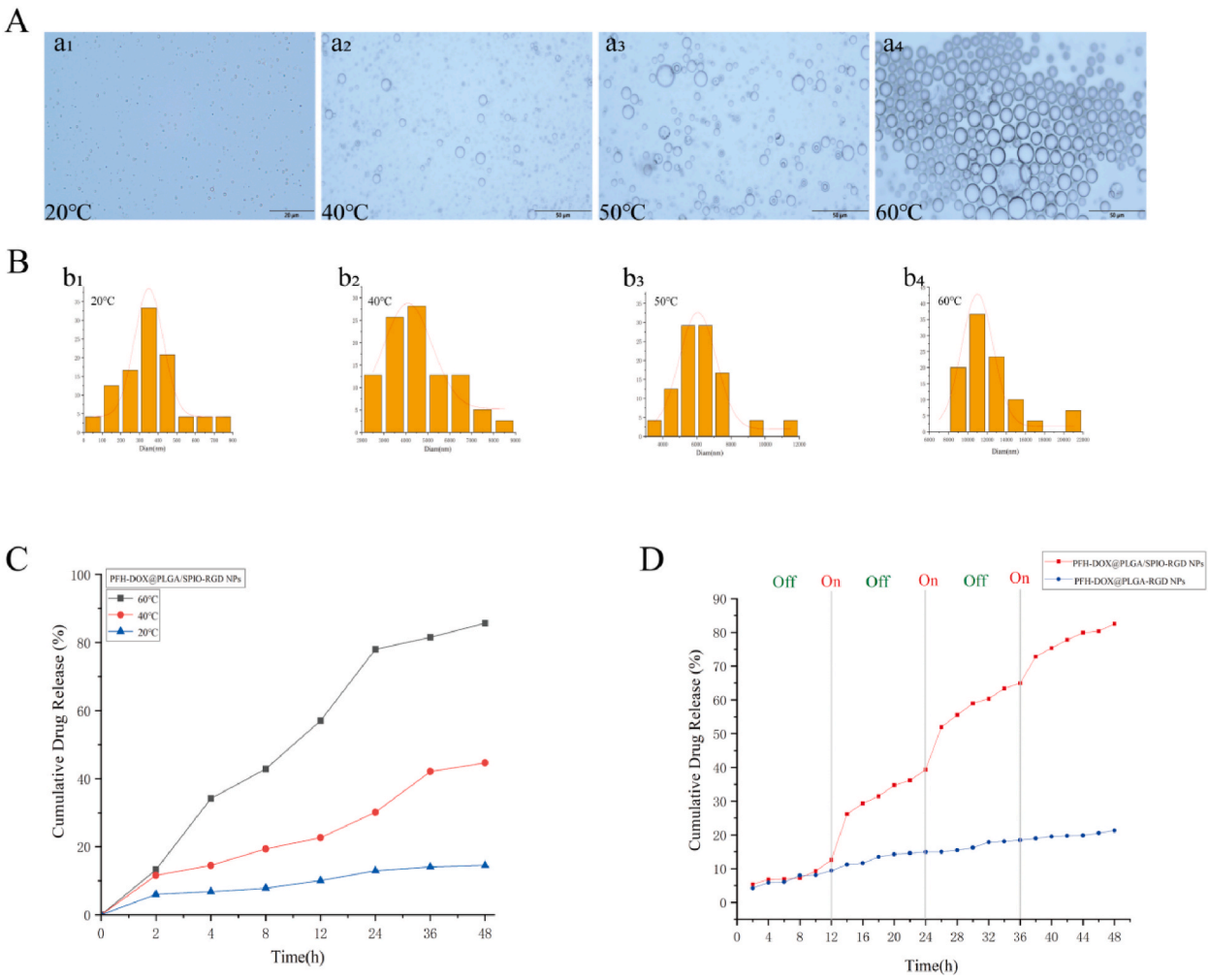

Fig. 5. Effect of NIR on the phase transition behavior of RNPS. A. Microscopic images of (a1-a4)NPs at temperatures of 20 °C, 40 °C, 50 °C, and 60 °C. B. Particle size variation trend of PFH gas microbubbles produced at different temperatures. C. NPs drug release curves at different temperatures for 48 h. D. Drug release profile of RNPS under multiple NIR laser irradiation.

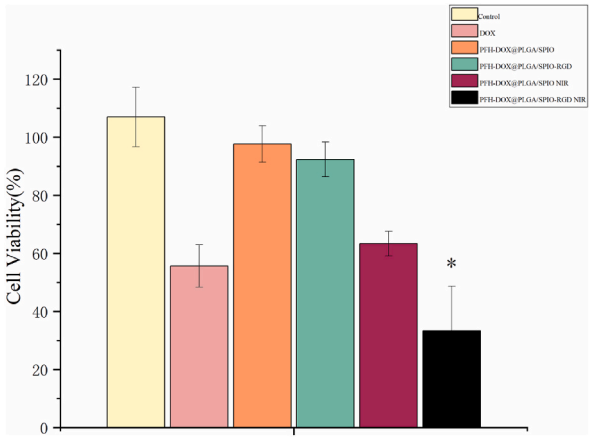

Fig. 6. Cytotoxicity studies of PBS, DOX, PFH-DOX@PLGA/SPIO NPs, RNPS, and RNPS after NIR irradiation. *$P < 0.05$.

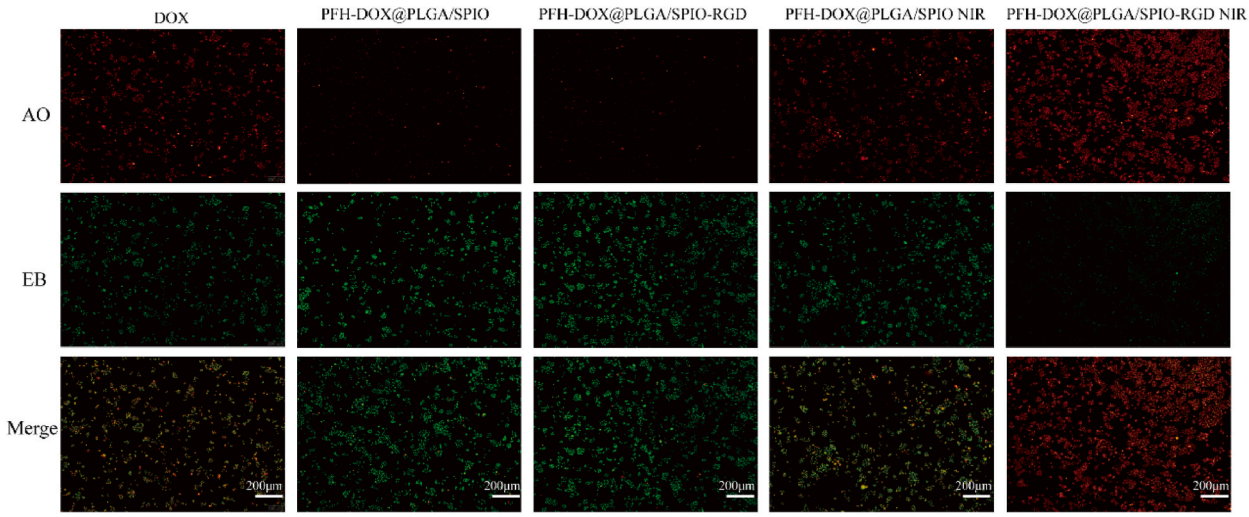

Fig. 7. Fluorescent staining of cell damage by DOX, PFH-DOX@PLGA/SPIO NPs, RNPS, and RNPS after NIR irradiation. (red: AO; Green: EB).

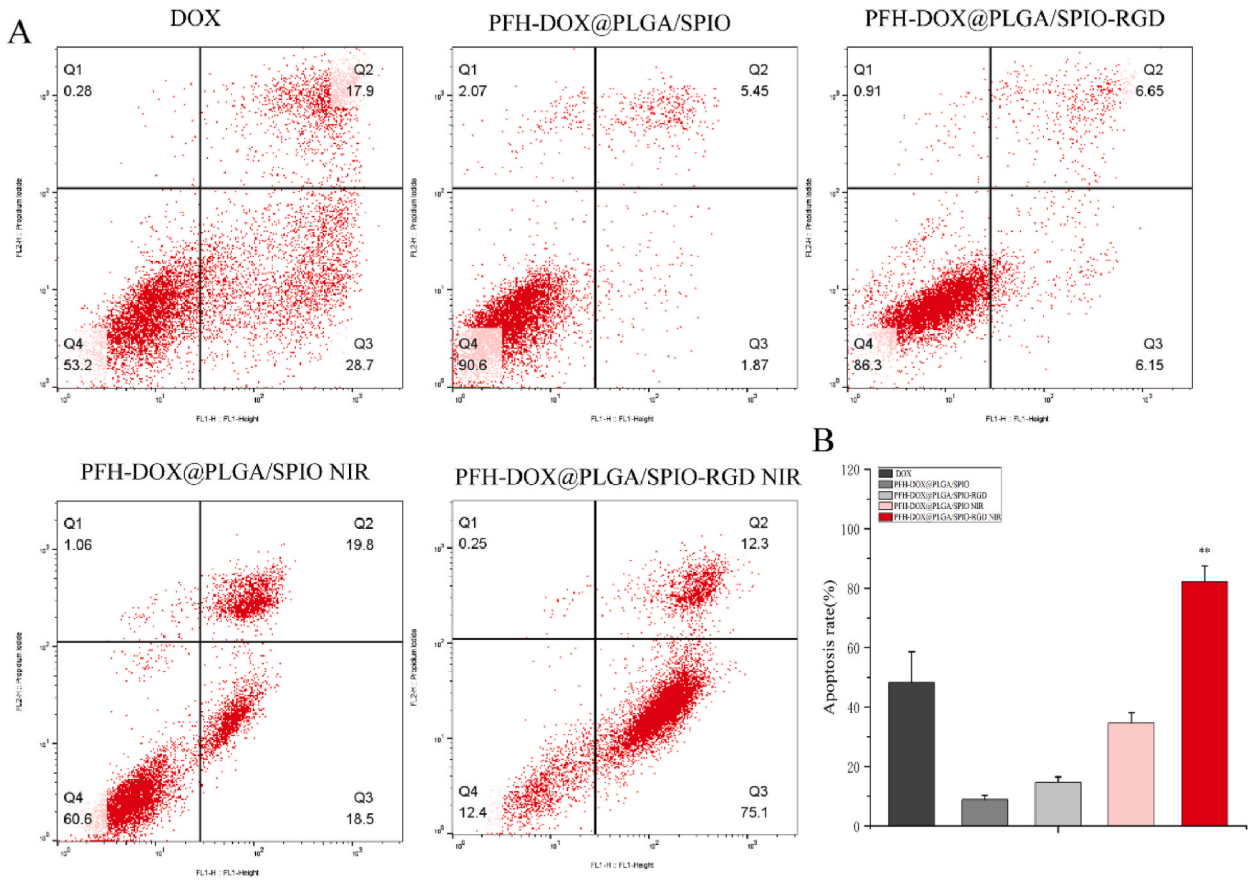

Fig. 8. Apoptosis Studies. A. Apoptosis mediated by PFH-DOX@PLGA/SPIO NPs and RNPS after DOX, PFH-DOX@PLGA/SPIO NPs, RNPS, and NIR irradiation. B. Apoptosis rate caused by different interventions. $^{**}P < 0.01$.

H&E results of each group after treatment showed that no significant abnormalities were found in major organs (liver, lung and kidney), indicating that NIR-mediated RNPs had good biosafety(Fig. 10). H&E results of all groups showed that PBS tumor cells almost did not apoptosis, PFH-DOX@PLGA/SPIO NPs and PFH-DOX@PLGA/Spio-RGD NPs had a certain degree of apoptosis, but the latter

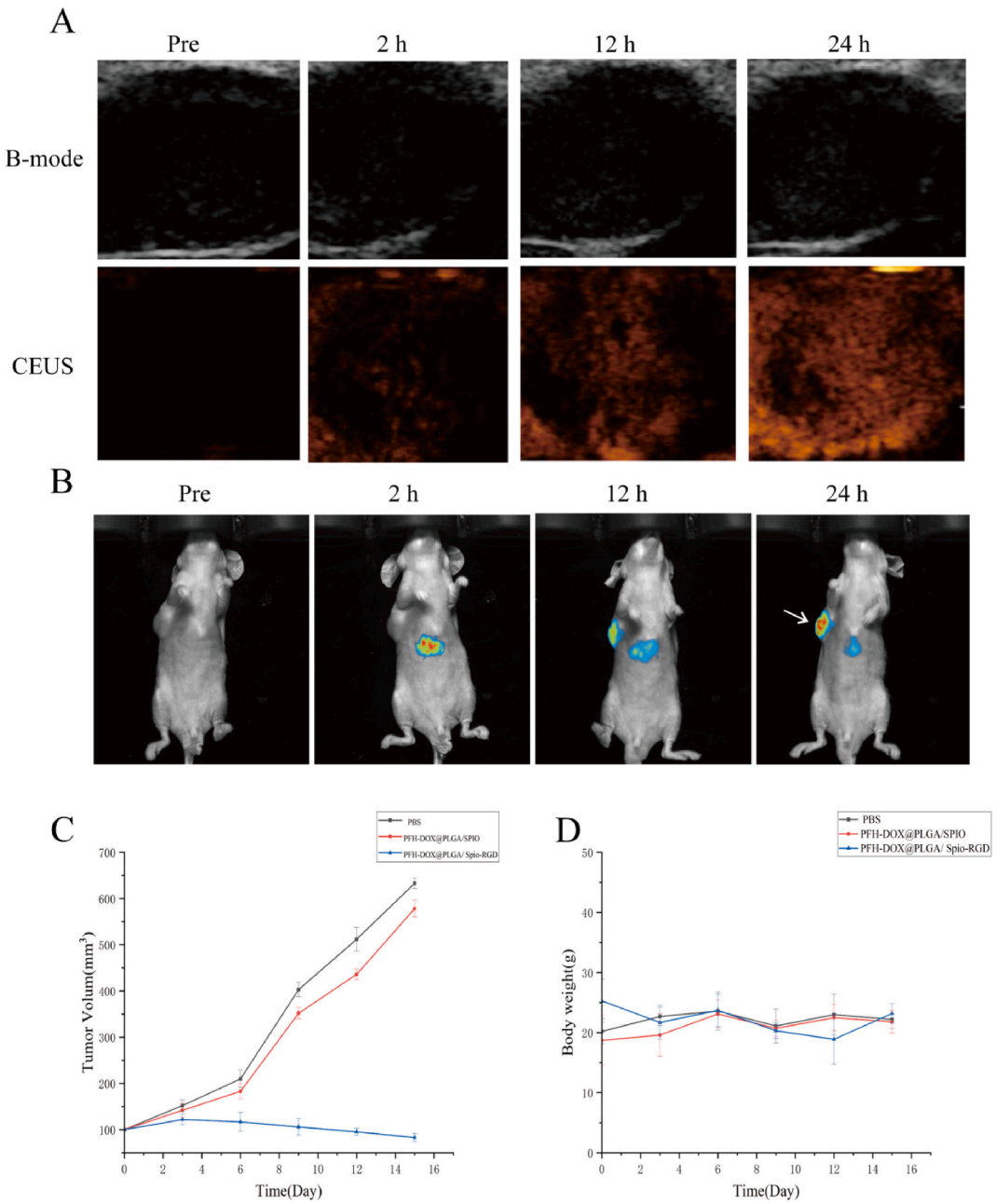

Fig. 9. In vivo targeted convergence of RNPS. A. Ultrasound imaging of tumor-bearing nude mice at different time points (2, 12, and 24 h) before and after NPs injection. B. Fluorescence imaging of nude mice with tumor after injection of PFH-DOX@PLGA/SPIO-RGD NPs into the tail vein before, 2h, 12h, and 24h postinjection. Arrows showed subcutaneous solid tumors of pancreatic cancer. C.Trend of tumor volume change. D. Trend of weight change of nude mice in each group.

was more severe.

4. Discussion

RNPS can combine the two imaging methods of ultrasound and Fluorescence imaging to obtain more accurate imaging diagnosis information. On the other hand, synergistic chemotherapy/photothermal therapy can be achieved. The experiments showed that the NPs were coated with a large amount of DOX and SPIO, which had excellent photothermal conversion ability and biological safety. The irradiation of near-infrared laser can not only promote the thermogenic phase transformation of internal PFH and realize enhanced ultrasound imaging, but also the photothermal effect and cavitation effect that occur in the irradiation process can make it expand or

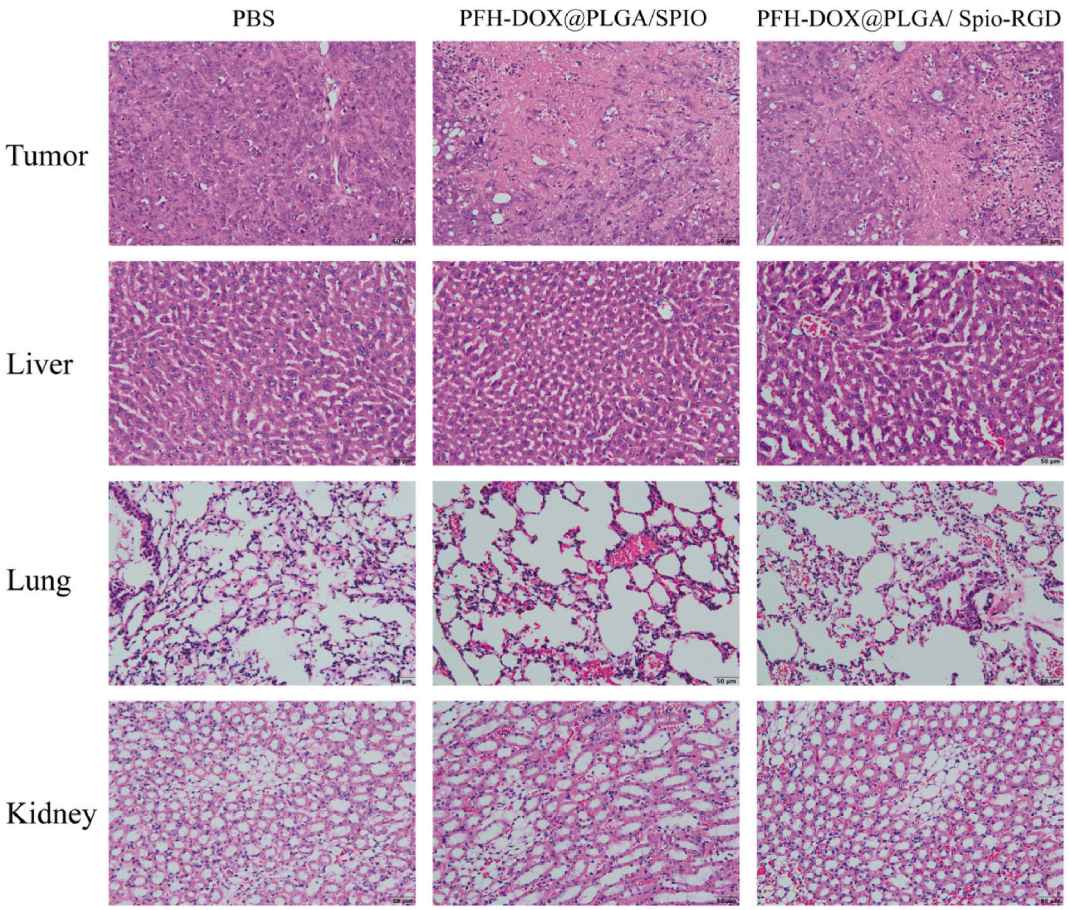

Fig. 10. H&E staining of tumor, liver, lung, kidney.

collapse, accelerate the release of internal drugs, and increase the permeability of tumor cell membrane, thereby improving the drug uptake of tumor cells and improving the therapeutic effect [25–27].

In this study, a targeted and multifunctional therapeutic nanosystem RNPS was successfully fabricated by encapsulation of PFH, SPIO, and DOX into PLGA and surface modification with RGD peptide. The RGD peptide conferred the ability of RNPS to target HPAC tumor cells. In cell experiments, the low apoptosis rate of RNPS demonstrated its excellent biocompatibility, while the cell inhibition rate of NIR-mediated NPs was stronger than that of DOX because RGD-modified NPs greatly improved the bioavailability of the drug and greatly improved the therapeutic effect of the drug. Under the action of the near-infrared laser, the photothermal transformation of SPIO inside PLGA converts PFH from liquid to gas and then forms the developing agent of the US. When the thermal effect exceeds the threshold, DOX is released from the broken NPs to achieve the purpose of targeted imaging therapy of tumors. In addition, it is precisely because of the good NIR absorption properties of SPIO that RNPS can be used as PA imaging agents. In a nude mouse model, RNPS demonstrated targeted and specific imaging of solid tumors of pancreatic cancer with prolonged retention time, demonstrating the great potential of this temperature-controlled dual imaging-guided drug delivery system for pancreatic cancer treatment. Under the guidance of US and PA dual-modality imaging, RNPS can be used as a specific drug delivery nanosystem and show a good targeting effect on pancreatic cancer, which provides a potential idea for the clinical treatment of tumors.

Ethics approval

This experiment was performed according to the protocol approved by the Animal Ethics Committee of Qiqihar Medical University (QMU-AECC-2022-116)

Consent to participate

Not applicable.

Consent for publication

Not applicable.

Availability of data and materials

All data generated or analyzed during this study are included in this published article.

CRediT authorship contribution statement

Shenglong Shi: Validation, Investigation, Data curation, Conceptualization. **Yingying Zhang:** Writing – original draft, Validation, Software, Resources, Formal analysis, Data curation. **Jian Huang:** Visualization, Validation, Software, Methodology, Conceptualization. **Zhengji Wang:** Visualization, Validation, Software, Methodology, Investigation, Conceptualization. **Weiyang Lv:** Visualization, Validation, Methodology, Investigation, Formal analysis. **Xing Li:** Visualization, Supervision, Resources, Project administration, Funding acquisition. **Ying Wang:** Validation, Supervision, Project administration, Methodology, Conceptualization. **Chunxin Huang:** Visualization, Validation, Software, Resources, Methodology, Formal analysis, Conceptualization. **Huilin Liu:** Writing – review & editing, Validation, Supervision, Project administration, Funding acquisition, Formal analysis, Data curation, Conceptualization.

Declaration of competing interest

The authors declare that they have no known competing financial interests or personal relationships that could have appeared to influence the work reported in this paper.

Acknowledgments

This research was supported by the Qiqihar science and technology plan joint guidance project (LSFGG-2023085), Clinical Research Foundation of Qiqihar Academy of Medical Sciences (No. QMSI2022L-05) and Heilongjiang Provincial Health Commission (No. 20220909020625).

References

[1] C.L. Wolfgang, J.M. Herman, D.A. Laheru, et al., Recent progress in pancreatic cancer, CA A Cancer J. Clin. 63 (5) (2013) 318–348.
[2] J.D. Mizrahi, R. Surana, J.W. Valle, et al., Pancreatic cancer, Lancet 395 (10242) (2020) 2008–2020.
[3] C. Springfeld, C.R. Ferrone, M.H.G. Katz, et al., Neoadjuvant therapy for pancreatic cancer, Nat. Rev. Clin. Oncol. 20 (5) (2023) 318–337.
[4] J. Wenfeng, W. Yushan, L. Rui, et al., Shape transformable strategies for drug delivery, Adv. Funct. Mater. 31 (18) (2021) 2009765, 2009765.
[5] O.C. Farokhzad, R. Langer, Impact of nanotechnology on drug delivery, ACS Nano 3 (1) (2009) 16–20.
[6] S. Bamrungsap, Z. Zhao, T. Chen, et al., Nanotechnology in therapeutics: a focus on nanoparticles as a drug delivery system, Nanomedicine (Lond) 7 (8) (2012) 1253–1271.
[7] J. Beik, Z. Abed, F.S. Ghoreishi, et al., Nanotechnology in hyperthermia cancer therapy: from fundamental principles to advanced applications, J. Contr. Release 235 (2016) 205–221.
[8] R. Wang, X. Wang, X. Mu, et al., Reducing thermal damage to adjacent normal tissue with dual thermo-responsive polymer via thermo-induced phase transition for precise photothermal theranosis, Acta Biomater. 148 (2022) 142–151.
[9] Y.L. Adam, C. Boreum, S. Taehoon, et al., In situ vaccination in lymphoma using photothermal therapy with CpG deoxynucleotide coated branched gold nanoparticles: analysis of tumor growth and immune response in a murine xenograft model, Blood 136 (Supplement 1) (2020) 20–21.
[10] L. Zhao, W. Yuan, H.P. Tham, et al., Fast-clearable nanocarriers conducting chemo/photothermal combination therapy to inhibit recurrence of malignant tumors, Small 13 (29) (2017) 1700963, 1700963.
[11] L. Xiaowei, An overview of doxorubicin in cancer therapy, J. Cancer Res. 10 (2021) 853–858.
[12] C. Liang, W. Chao, F. Liangzhu, et al., Functional nanomaterials for phototherapies of cancer, Chem. Rev. 114 (21) (2014) 10869–10939.
[13] C.V. Rocha, V. Gonçalves, M.C. da Silva, et al., PLGA-based composites for various biomedical applications, Int. J. Mol. Sci. 23 (4) (2022 Feb 12) 2034–2067.
[14] Z. Ruirui, H. Jian, X. Xihui, et al., PLGA-based drug delivery system for combined therapy of cancer: research progress, Mater. Res. Express 8 (12) (2021) 122002, 122002.
[15] J. Huang, Z. Wang, Z. Chen, et al., Ultrasound-mediated multifunctional magnetic microbubbles for drug delivery of celastrol in VX2 liver transplant tumors, Drug Deliv Transl Res 14 (2) (2024) 555–570.
[16] L. Deng, X. Cai, D. Sheng, et al., A laser-activated biocompatible theranostic nanoagent for targeted multimodal imaging and photothermal therapy, Theranostics 7 (18) (2017) 4410–4423.
[17] X. Shen, T. Li, Z. Chen, et al., Luminescent/magnetic PLGA-based hybrid nanocomposites: a smart nanocarrier system for targeted codelivery and dual-modality imaging in cancer theranostics, Int. J. Nanomed. 12 (2017) 4299–4322.
[18] T.S. Adina, C. Maria-Viorica, P. Paulina, et al., PLGA-gentamicin and PLGA- hydroxyapatite-gentamicin microspheres for medical applications, Pharmaceut. Chem. J. 56 (5) (2022) 645–653.
[19] T.M. Mandana, S. Yosi, K. Hiroto, et al., Targeted drug delivery strategies for precision medicines, Nat. Rev. Mater. 6 (4) (2021) 351–370.
[20] L. Yan, Y. Hang, Z. Yifan, et al., Dual and multi-targeted nanoparticles for site-specific brain drug delivery, J. Contr. Release 317 (2020) 195–215.
[21] S. Kosar, A.F. Michelle, H. Swati, et al., Mechanical, rheological and anaerobic biodegradation behavior of a Poly(lactic acid) blend containing a Poly(lactic acid)-co-poly(glycolic acid) copolymer, Polym. Degrad. Stabil. 170 (2019) 109018, 109018.
[22] Wu Xing, Dual AO/EB staining to detect apoptosis in osteosarcoma cells compared with flow cytometry, Medical science monitor basic research 21 (2015) 15–20.
[23] T. Rohit Singh, E. Devaraj, Lagerstroemia speciosa(L.) Pers. triggers oxidative stress mediated apoptosis via intrinsic mitochondrial pathway in$HepG_2$ cells, Environ. Toxicol. 35 (11) (2020) 1225–1233.
[24] E.M. Rahime, F. Bahareh, K. Ali, Synthesis, characterization, biomedical application, molecular dynamic simulation and molecular docking of schiff base complex of Cu(II) supported on Fe_3O_4/SiO_2/APTS, Int. J. Nanomed. 15 (2020) 2583–2603.

[25] S.M. Lee, H. Park, K.H. Yoo, Synergistic cancer therapeutic effects of locallydelivered drug and heat using multifunctional nanoparticles, Adv. Mater. 22 (36) (2010) 4049–4053.
[26] M.L. Viger, W. Sheng, K. Doré, et al., Near-infrared-induced heating of confined water in polymeric particles for efficient payload release, ACS Nano 8 (5) (2014) 4815–4826.
[27] S. Mura, J. Nicolas, P. Couvreur, Stimuli-responsive nanocarriers for drug delivery, Nat. Mater. 12 (11) (2013) 991–1003.